



Prediction model of water yield property based on GRA, FAHP and TOPSIS methods for Ordovician top aquifer in the Xinwen coalfield of China

Mei Qiu¹ · Fengjun Huang¹ · Ying Wang¹ · Tao Guan¹ · Longqing Shi¹ · Jin Han²

Received: 30 August 2018 / Accepted: 27 April 2020 / Published online: 10 May 2020
© Springer-Verlag GmbH Germany, part of Springer Nature 2020

Abstract

In North China, the exploitation of deep coal seams is seriously threatened by water inrush from Ordovician limestone. Predicting the water yield property of the Ordovician limestone aquifer has been an important and challenging task. Based on accessible geological and hydrological data, a water yield property index (WYPI) model, which integrated four factors including the water inflow of borehole, fault impact factor, drilling fluid consumption and burial depth of the Ordovician top aquifer, was proposed for predicting the spatial distribution of the water yield property of the upper Majiagou group limestone in the Ordovician top (Ordovician top aquifer) in the Xinwen coalfield, Shandong, China. The grey relative analysis (GRA) and fuzzy analytic hierarchy process (FAHP) methods were combined to objectively determine the weights of each factor. Then, the technique for order performance by similarity to ideal solution and the weights calculated by the GRA and FAHP were used to establish the WYPI model. The water yield property zone map, which was built using the WYPI values, displayed three water yield property zones. The WYPI model was further verified by taking into account practical engineering data, which were considered effective in predicting the zonation of the water yield property of the Ordovician top aquifer in the Xinwen coalfield, Shandong, China.

Keywords Water yield property zone · Ordovician top aquifer · Karst · Coalmine · China

Introduction

China possesses substantial coal resources, while the hydrogeological conditions of mining are among the most complicated in the world (Li et al. 2018; Wu et al. 2011b; Yin et al. 2019; Zhao et al. 2018). In North China, Permo-Carboniferous coal seams are mined underground, and the thick Ordovician limestone strata containing an abundant supply of water are often formed below the bottom of the Permo-Carboniferous coal-bearing formations (Wang and Shi 2019; Xu et al. 2019). The Ordovician limestone aquifer acts as

the main source of water recharge. Karst water hazards from the Ordovician limestone aquifer pose a severe threat to the exploitation of deep coal seams in North China-type coalfields, causing equipment damage, project delays, and even casualties (Bu et al. 2019; Sun et al. 2015; Wang and Meng 2018; Zhang et al. 2017). Water inrush is controlled by multiple factors, such as water pressure, water yield property, geological structures, floor aquifuge, and mining conditions (Li et al. 2015; Wu et al. 2017b; Zhao et al. 2014), among which the water yield property is an essential factor that refers to the productivity (quantity and duration) of the aquifer (Qiu et al. 2017; Yin et al. 2018). The severity of water hazards depends on the water yield property (Wu et al. 2011a, b). It will not cause substantial harm, even if water passage can reach an aquifer in a poor water yield property region during mining, however, it is more likely to cause serious water inrush in a rich water yield property zone (Qiu et al. 2017; Wu et al. 2017a, c). Hence, an objective and comprehensive assessment of the water yield property of an aquifer is essential for safely mining in deep coal seams and managing the mining (Wu 2014; Shi et al. 2019c).

✉ Longqing Shi
cattony2002@126.com

¹ Shandong Provincial Key Laboratory of Depositional Mineralization and Sedimentary Minerals, College of Earth Sciences and Engineering, Shandong University of Science and Technology, Qingdao 266590, China

² College of Computer Science and Engineering, Shandong University of Science and Technology, Qingdao 266590, China

Specific field (represented by q) has been widely used to evaluate the water yield property of aquifers in China based on regulations for mine water prevention and control (State Administration of Work Safety and State Administration of Coal Mine Safety 2009), which is defined as water production of boreholes per meter of drawdown during pumping tests operated in surface boreholes. However, the operability of this specific field method is minimal in practice because of the absence of borehole data from a pumping test in the Ordovician limestone aquifer which costs a lot. As a result, a scientific and accurate partition map of the water yield property of the Ordovician limestone aquifer drawn using q is difficult to achieve. The assessment of the water yield property will be greatly limited if we only consider the specific yield. Another traditional approach to evaluating the water yield property of aquifers is the geophysical method (Gao et al. 2019; Shi et al. 2019b). These traditional approaches are usually time-consuming and expensive. Hence, it is of great management importance to develop an effective assessment method of the water yield property with the available geological and hydrogeologic data.

Recently, numerous scholars and coal workers have devoted themselves to the research and approach emerged one after another. A water-richness index method that has been widely promoted was proposed based on the analytic hierarchy process by a geographic information system to evaluate the water yield property of aquifers (Wu et al. 2011a; Yan 2015; Yin et al. 2018). A fuzzy analytic hierarchy process has been used to analyze the water yield property based on GIS (Han et al. 2012; Yang et al. 2017). These methods provide a powerful tool for predicting the water yield property of aquifers, but at the same time, the methods are not appropriate because the weights of the controlling factors are obtained by the analytic hierarchy process, which is relatively subjective (Wu et al. 2017c). To address this disadvantage, weighted grey relational degree theory and the fuzzy analytic hierarchy process were used to evaluate the water yield capacity of a fracture aquifer (Xu et al. 2016; Wu et al. 2017c). These methods provided good results, but the models were linearly weighted. In addition, numerical modeling was used to predict the permeability of the fracture networks (Mourzenko and Thovert 2011), and remote sensing technology and geographic information system modeling were used to map the groundwater potential zones (Dar et al. 2010). However, with the buried depth increasing of the fracture aquifer, these approaches are not always applicable because they are restricted by topography and geomorphology, and the degree of hydrogeological exploration of new mining areas is usually low. Thus, the use of accessible geological and hydrogeologic data to assess aquifer water yield property is a necessary and challenging task.

Accordingly, this paper proposed an innovative method predicting the water yield property of aquifers using

accessible geological and hydrological data based on the grey relative analysis (GRA), fuzzy analytic hierarchy process (FAHP), and the technique for order performance by similarity to ideal solution (TOPSIS), applied to predict the water yield property of the upper Majiagou group limestone in the Ordovician top (Ordovician top aquifer) in the Xinwen coalfield, Shandong, China. The GRA and FAHP methods were combined to determine the weights of the assessment factors, a process that helps decrease the subjectivity of traditional expert analysis based on the data of the factors and q . Thus, the TOPSIS method, an effective nonlinear multicriteria decision-making method for ranking performance of the technique based on similarity to an ideal solution, was then applied to establish a water yield property index (WYPI) model. Finally, the relatively poorer or richer water yield property zones were predicted by the WYPI model, which provided a scientific and reasonable partition map of the water yield property of the Ordovician top aquifer.

Study area

Geological conditions

The Xinwen coalfield lies in the midwestern part of Shandong Province, China, where there are seven main coalmines from west to east: Shengquan, Xiezhuang, Zhaizhen, Liangzhuang, Suncun, Huayuan, and Huaheng coalmines. This paper focuses on the Xiezhuang, Zhaizhen, and Liangzhuang coalmines, and the study area is shown in Fig. 1. The Xinwen coalfield is a typical North China coalfield of the Permo-Carboniferous period. The coal-bearing strata consist of the Benxi Formation (F), Taiyuan F, Shanxi F, and Shihezi F, from bottom to top. The mined coal seams belong to Taiyuan F and Shanxi F, of which nos. 2, 4, 6, 11, 13 and 15 are minable seams. The coal-bearing strata are covered by the Jurassic System (S) (developed locally in the south of the F₁₀ fault), Paleogene S, and Quaternary S. The sedimentary basement of the coal-bearing strata is Ordovician S.

The Xinwen coalfield is a faulted and folded monocline dipping NNE, with gentle dips less than 30°. Generally, the faults are well developed in the area. The major faults are oriented NW, NEE, and NE, and others are oriented NNW. In particular, the Lianhuashan fault, oriented NW, forms the north border of the coalfield, and the no. 10 fault (F10 in Fig. 1) and its branch faults, in the NW direction, cut the Xinwen coalfield into a south zone and a north zone.

Hydrogeological conditions

The Xinwen coalfield is located in the sunken area between the Lianhuashan and Mengshan Mountains. The main surface water system is the Chaiwen River and its branches,

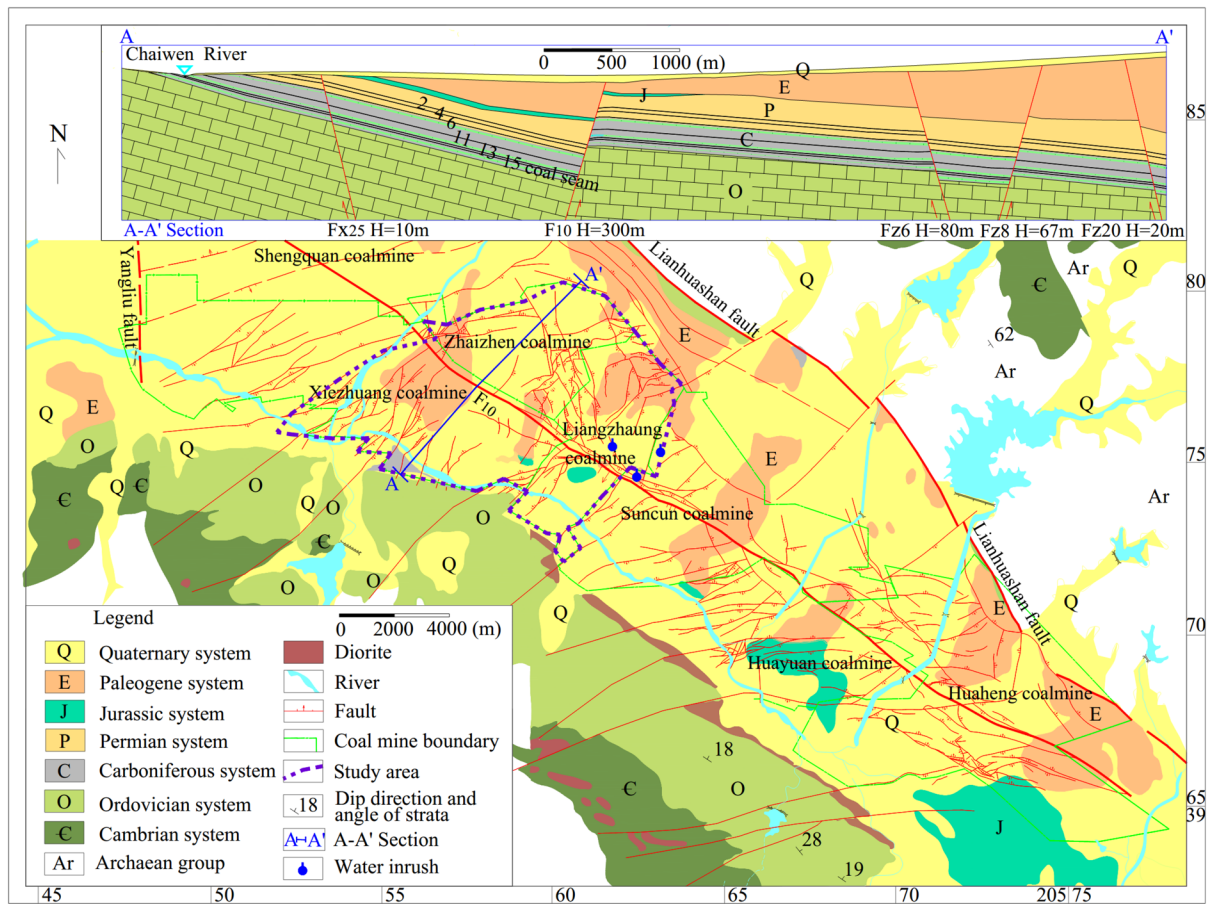


Fig. 1 Geological and structural map of the study area

which flow through the coalfield east to west. The aquifers of the area are mainly the water-bearing gravel layer of the Quaternary S, the gravel-stone layer aquifer of Paleogene S, the sandstone fractured aquifers of the Permo-Carboniferous S, the thin limestone aquifers of the Carboniferous Taiyuan F, and the Ordovician limestone karst-fractured aquifer, forming a multilayer structural groundwater system.

After 60 years of coal mining in the Xinwen coalfield, deep coal seams have formed, mainly the nos. 11, 13 and 15 coal seams. The Ordovician limestone aquifer seriously threatens the mining production of the nos. 11, 13, 15 coal seams. Vertically, the thickness of the Ordovician limestone of the coalfield in northern China varies greatly. For the Xinwen coalfield, the thickness of the Ordovician limestone strata is greater than 800 m. Vertically, many paleokarst systems formed and evolved in the Ordovician limestone strata in the process of geological evolution, but karst-fractured groundwater developed in the Ordovician top aquifer has had an impact on production safety. Therefore, the proposed study focuses on the Ordovician top aquifer.

South of the coalfield are mountains of Ordovician limestone and Cambrian limestone, where the Ordovician

limestone, exposed to the surface, is mainly recharged by rainfall. The north border of the coalfield is the Lianhuashan fault (the throw of the fault is more than 3000 m). The foot-wall of the Lianhuashan fault is gneiss of the Pre-Sinian S of the Archaean group, cutting off the recharge of the aquifers in the Xinwen coalfield by rainfall. Only in the local area south of the Lianhuashan fault is Ordovician limestone exposed on the surface. However, in the Xinwen coalfield, the Ordovician limestone is covered by coal-bearing strata and Paleogene strata, which cut off the hydraulic relationship between the Ordovician limestone aquifer and the water on the surface, the water-bearing gravel layer of the Quaternary S, and the gravel-stone layer aquifer of the Paleogene S. With the increase in the burial depth of the Ordovician limestone from south to north in the Xinwen coalfield, the recharge conditions of the groundwater of the Ordovician limestone aquifer are gradually becoming limited (Fig. 1).

Because Ordovician limestone is buried deep underground, detecting the location and water yield property of the Ordovician top aquifer is restricted. In general, the specific field, obtained by a pumping test of the surface borehole, is used to evaluate the water yield property of

aquifers in China. In the study area, seven pumping tests of the Ordovician top aquifer were carried out, mostly in the central and southern study areas. According to the regulations for mine water prevention and control (State Administration of Work Safety and State Administration of Coal Mine Safety 2009), the water yield property of aquifers can be defined by four categories: poor water yield property when $q \leq 0.1$ L/s m; medium water yield property when $0.1 \text{ L/s m} < q \leq 1.0$ L/s m; rich water yield property when $1.0 \text{ L/s m} < q \leq 5.0$ L/s m; and very rich water yield property when $q > 5.0$ L/s m. Accordingly, the water yield property of the Ordovician top aquifer in the study area can be assessed based on q as shown in Fig. 2. The water yield property of the Ordovician top aquifer in the southwestern part of the study area was classified as rich, in the north-central part as medium, and the eastern part as poor. However, three water inrushes from the underlying Ordovician top aquifer occurred during mining the nos. 11 and 13 coal seams in the poor water yield property zone based on q , and their water inflow rates were as high as 772.2 m³/h, 1920 m³/h, and 78 m³/h. The occurrence of water inrushes clearly was the opposite of having partitions of the water yield property based on q because large-scale water inrush is impossible in poor water yield property zones during mining. Therefore, it is necessary to objectively and comprehensively assess the water yield property of the Ordovician top aquifer for safely mining in deep coal seams.

Data

Selected relevant factors of the water yield property of Ordovician top aquifer

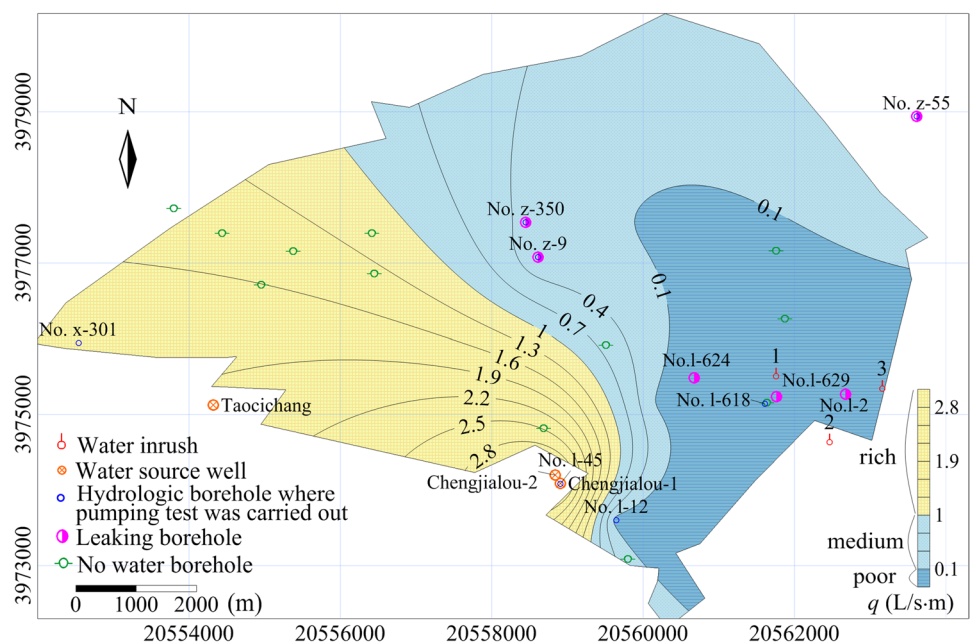
Usually, the water yield property of the Ordovician limestone aquifer is mainly controlled by the storage space of water, the quantity of water in the storage space and the water supply. The main potential water yield property conditioning factors in this study are the water inflow of borehole (WIB), fault impact factor (FIF), drilling fluid consumption (DFC) and burial depth (BD) of the Ordovician top aquifer. These hydrologic and geologic data were gathered from boreholes and seismic exploration before and during mining.

Relevant factors

Water inflow of borehole (WIB)

The water inflow of boreholes is the most direct indicator of an aquifer water yield property, which is the maximum water gushing when leaving the Ordovician limestone strata. The larger the value of WIB is, the richer the water is. During mining the nos. 11, 13, and 15 coal seams, supplementary hydrogeological explorations of the Ordovician top aquifer were carried out. Ninety underground hydrogeologic boreholes were drilled into the Ordovician limestone aquifer to explore the conditions of the Ordovician top aquifer in the study area. The WIB was obtained by observing the value of each underground hydrogeologic

Fig. 2 Water yield property zone map of the Ordovician top aquifer based on q



borehole, and then, the contour map of WIB in the Ordovician top aquifer was drawn as shown in Fig. 3a. The change in WIB was large in the study area. In the south-central and north-central regions, the WIB was larger than that in the other regions.

Fault impact factor (FIF)

Water in the Ordovician limestone strata mainly exists in fractures. Faults have a great influence on groundwater storage and migration, which is closely related to the groundwater potential (Mourzenko and Thovert 2011; Yin et al. 2018). The analysis of water inrush indicates that rock is more crushed and fractured at the intersections and endpoints of faults than at other areas of faults because of the concentration of ground stress (Shi et al. 2019a; Yin et al. 2018). The fractured zone further develops and

forms the main space for accumulating groundwater in the fractured aquifer (Wu et al. 2011a). The greater number of and larger the faults are, the more space for storage and conduction of groundwater (Yin et al. 2018). Therefore, the intersections and endpoints of faults, extension length, and fault throw were taken into account by the fault impact factor to evaluate the development degree of a fracture. The fault impact factor is calculated as follows:

$$FIF = \frac{\sum_i^n l_i h_i}{S} + M, \tag{1}$$

where FIF is the fault impact factor; h is the fault throw; l is the corresponding strike length; S is the area of the grid cell; n is the number of faults encountered in the grid cell; M is the normalization value of fault intersections and endpoints. According to fault distribution characteristics, the study area was organized into 500 m × 500 m grid cells, and then, the

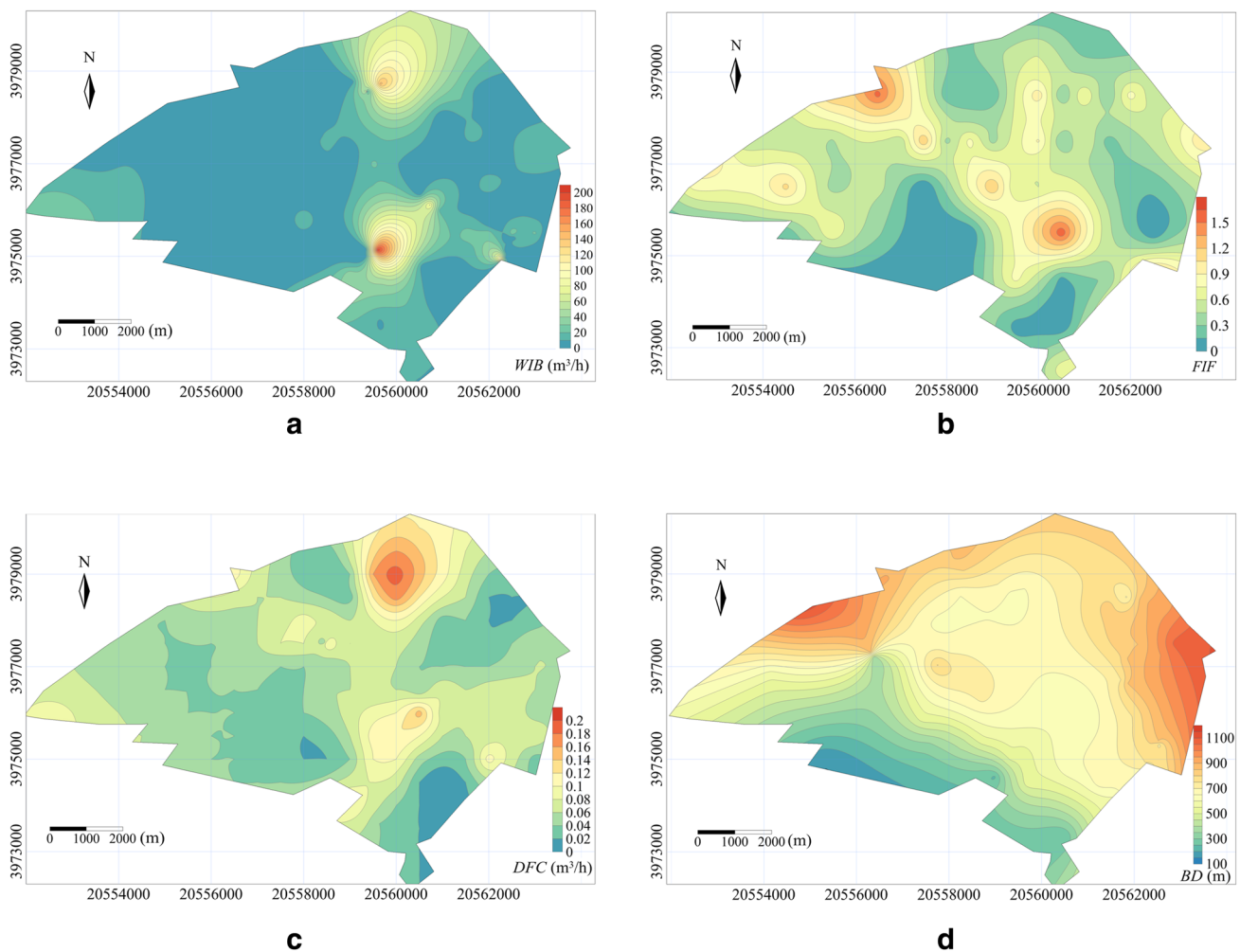


Fig. 3 Thematic maps of every relevant parameters

fault intersections and endpoints, and fault throw and its corresponding strike length were counted in each grid cell to calculate FIF. A contour map of FIF is shown in Fig. 3b.

Drilling fluid consumption (DFC)

When boreholes are drilled into an aquifer, drilling fluid consumption will clearly increase. Differences in consumption indicate the distinction of cracks in terms of development degree and connectivity. The DFC is an index that reflects the connectivity of the crack and permeability of an aquifer (Wu et al. 2008). The DFC was obtained by observing the value in each exploratory borehole, and the contour map of DFC was drawn by Golden Software Surfer 13.0 as shown in Fig. 3c.

Burial depth (BD)

The burial depth of the Ordovician top aquifer is related to the water supply. With the increase in the burial depth, the recharge conditions become gradually limited in the study area. In addition, the lithostatic pressure increases with increasing depth, as does the degree of crack compaction, which decreases the connectivity slightly by possibly closing the fractures present. The burial depth of the Ordovician top was acquired from geoexploration, 3D-seismic exploration, and workface construction, and its contour map is shown in Fig. 3d.

Methodology

Procedures

Predicting the water yield property potential zone of the Ordovician top aquifer included four main steps: (a) selecting the relevant factors of the water yield property and data collection, (b) determining the evaluation factor weights, (c) establishing the water yield property index model, and (d) validating and applying the results.

Determination of the factor weights

The fuzzy analytic hierarchy process is a fuzzy group decision-making method that comprehensively uses fuzzy assessment and an analytic hierarchy process. This interactive determination process enables decision makers to fully participate in the determination and analysis of weights. However, there are similarities between the traditional analytic hierarchy process and fuzzy analytic hierarchy process; the relative importance of the evaluation factors was determined by experts based on the Saaty rating scale, and the data were subjective and did not have a scientific basis. To avoid these disadvantages, the GRA method was applied to improve the traditional FAHP method.

Calculation of the comparison matrix based on the GRA method

GRA is a significant part of the grey system theory that professor Deng created, which is a simple and scientific process used to determine relevancy between evaluation factors and a target (Deng 1982, 1989). This method is used to judge the degree of the relationship based on the geometrical distance between the reference sequence (specific field *q* reflecting the water yield property) and the compared sequences (the evaluation factors including WIB, FIF, DFC and BD). The data of *q* and the evaluation factors in seven hydrologic boreholes were collected where pumping tests were carried out in the study area (Table 1).

To eliminate the impact of the different dimensions of the original data, the compared sequences were normalized using the following formula:

$$x_t^{(1)}(i) = x_t^{(0)}(i) / \left[\frac{1}{n} \sum_{t=1}^n x_t^{(0)}(i) \right], \tag{2}$$

where $i = 1, 2, \dots, m, t = 1, 2, \dots, n; x_t^{(0)}(i)$ is the original data of the *i*th evaluation factor in the *t*th hydrologic borehole. The reference sequence $x_t^{(0)}(0)$ was normalized as follows:

Table 1 Data of *q* and the evaluation factors in seven hydrologic boreholes

No.	Hydrologic boreholes	Compared sequences				Reference sequence <i>q</i> (L/s m)
		WIB (m ³ /h)	FIF	DFC (m ³ /h)	BD (m)	
1	No. l-12	9	0.14	0.04	310	0.0009
2	No. l-618	15	0.46	0.05	695	0.00285
3	No. l-45	33	0.45	0.11	295	3.54
4	No. x-301	30	0.4	0.09	540	1.743
5	No. z-9	10	0.75	0.05	705	0.18
6	No. z-350	15	0.7	0.05	690	0.332
7	No. z-55	13	0.66	0.07	940	0.386

Table 2 Relative importance of the evaluation factors based on GRA method

Evaluation factors	Pumping test (PT)						
	1st PT (P 1)	2nd PT (P 2)	3rd PT (P 3)	4th PT (P 4)	5th PT (P 5)	6th PT (P 6)	7th PT (P 7)
WIB (F_1)	0.866	0.715	0.423	0.999	0.955	0.888	1.000
FIF (F_2)	1.000	0.745	0.392	0.668	0.648	0.716	0.758
DFC (F_3)	0.875	0.806	0.443	0.877	0.900	1.000	0.864
BD (F_4)	1.000	0.780	0.432	0.806	0.832	0.897	0.786

Table 3 Group fuzzy comparison matrix B

B	F_1	F_2	F_3	F_4
F_1	(1.000, 1.000, 1.000)	(0.866, 1.049, 1.273)	(0.866, 1.182, 1.495)	(0.887, 1.006, 1.157)
F_2	(0.669, 0.846, 1.155)	(0.779, 0.887, 1.000)	(1.000, 1.000, 1.000)	(0.716, 0.850, 1.143)
F_3	(0.864, 0.994, 1.127)	(0.875, 1.043, 1.115)	(0.875, 1.176, 1.396)	(1.000, 1.000, 1.000)
F_4	(0.786, 0.953, 1.155)	(1.000, 1.000, 1.000)	(1.000, 1.127, 1.284)	(0.897, 0.959, 1.143)

$$x_t^{(1)}(0) = x_t^{(0)}(0) / \left[\frac{1}{n} \sum_{i=1}^n x_t^{(0)}(0) \right]. \tag{3}$$

After normalization, the grey relational coefficients between the evaluation factors and q were solved to determine the influencing degree of the evaluation factors for the water yield property using the following formula (Deng 1989):

$$r_{i,0} = \frac{\Delta_{\min} + \xi \Delta_{\max}}{\Delta_{i,0}(i) + \xi \Delta}, \tag{4}$$

where $\Delta_{\max} = \max_{v_i} \max_{v_t} |x_t^{(1)}(i) - x_t^{(1)}(0)|$ is the absolute maximum difference and $\Delta_{\min} = \min_{v_i} \min_{v_t} |x_t^{(1)}(i) - x_t^{(1)}(0)|$ is the minimum difference; $\Delta_{i,0}(i) = |x_t^{(1)}(i) - x_t^{(1)}(0)|$ is the absolute difference of the i th hydrologic borehole between the i th evaluation factor and the specific field q . $\xi \in [0, 1]$ is the resolution coefficient, and the value is 0.5 in this study.

According to the GRA method, each evaluation factor's grey relational coefficient of the seven pumping tests was calculated indicating the influencing degree on the aquifer water yield property. The relative importance of the evaluation factors based on the GRA method is shown in Table 2.

Table 4 Group fuzzy weights and total weights of each evaluation factor

Evaluation factor	Group fuzzy weight	Total weight
F_1	(0.197, 0.264, 0.348)	0.262
F_2	(0.171, 0.223, 0.306)	0.227
F_3	(0.197, 0.262, 0.329)	0.257
F_4	(0.200, 0.251, 0.326)	0.254

Based on the relative importance of the evaluation factors above as shown in Table 2, we established seven 4×4 pair-wise comparison matrixes based on the following equation:

$$A = \begin{pmatrix} 1 & a_{12} & a_{13} & a_{14} \\ 1/a_{12} & 1 & a_{23} & a_{24} \\ 1/a_{13} & 1/a_{23} & 1 & a_{34} \\ 1/a_{14} & 1/a_{24} & 1/a_{34} & 1 \end{pmatrix}, \tag{5}$$

where $a_{ij} = F_i/F_j$ represents a judgment of the relative importance of factors F_i and F_j .

Determination of the total weight based on the FAHP method

First, group fuzzy comparison matrix B was generated (Table 3) based on pair-wise comparison matrixes using a fuzzy triangular number (Ataei et al. 2012):

$$B = \begin{pmatrix} (1, 1, 1) & (\alpha_{12}, \beta_{12}, \gamma_{12}) & (\alpha_{13}, \beta_{13}, \gamma_{13}) & (\alpha_{14}, \beta_{14}, \gamma_{14}) \\ 1/\gamma_{12}, 1/\beta_{12}, 1/\alpha_{12} & (1, 1, 1) & (\alpha_{23}, \beta_{23}, \gamma_{23}) & (\alpha_{24}, \beta_{24}, \gamma_{24}) \\ 1/\gamma_{13}, 1/\beta_{13}, 1/\alpha_{13} & 1/\gamma_{23}, \beta_{23}, 1/\alpha_{23} & (1, 1, 1) & (\alpha_{34}, \beta_{34}, \gamma_{34}) \\ 1/\gamma_{14}, 1/\beta_{14}, 1/\alpha_{14} & 1/\gamma_{24}, 1/\beta_{24}, 1/\alpha_{24} & 1/\gamma_{34}, 1/\beta_{34}, 1/\alpha_{34} & (1, 1, 1) \end{pmatrix}, \tag{6}$$

where $(\alpha_{ij}, \beta_{ij}, \gamma_{ij})$ is the fuzzy triangular number, and $\alpha_{ij} \leq \beta_{ij} \leq \gamma_{ij}$; α_{ij} , β_{ij} , and γ_{ij} indicate the lower bound, the geometric mean, and the upper bound, respectively.

Then, using the fuzzy algorithm, the group fuzzy weight of any evaluation factor (Table 4) was calculated based on the data in Table 3 using the following equation:

$$w_i = r_i \otimes (r_1 \oplus r_2 \oplus r_3 \oplus r_4)^{-1}, \tag{7}$$

$$r_i = (b_{i1} \otimes b_{i2} \otimes b_{i3} \otimes b_{i4}), \tag{8}$$

where operators \oplus and \otimes denote the addition and multiplication of fuzzy numbers, respectively; $w_i = (w_i^L, w_i^M, w_i^U)$ represents the fuzzy weight vector of the i th factor; $i = 1, 2, \dots, 4$.

Finally, we obtained the total weights of each evaluation factor by defuzzification and normalization, as shown in Table 4.

Establishment of the water yield property index model

In this paper, we use a nonlinear method, the TOPSIS method, to assess the water yield property of the aquifer. TOPSIS is an evaluation method used to solve multicriteria decision-making problems and was originally developed by Hwang and Yoon (1981). The WYPI model was established using the TOPSIS method based on the values of factors and the weights calculated by GRA and FAHP methods. According to the TOPSIS method, we can first construct one imaginary sample with the richest water yield property, which is defined as a positive ideal solution (PIS), and one imaginary sample with the poorest water yield property, which is defined as a negative ideal solution (NIS). The richest sample of all the assessment samples is the one that has the nearest distance to the positive ideal solution and is farthest from the negative ideal solution, and the poorest sample of all the assessment samples is the one that has the nearest distance to PIS and is farthest from NIS. Then, the distances of each sample to the negative and positive ideal solutions were calculated to establish the water yield property index model, with which we can rank the relative water yield property values of the assessment samples in the study area. Based on the TOPSIS theory, the water yield property index model was conducted as follows:

First, the study area was organized into 500 m × 500 m grid cells using latitudinal and longitudinal lines. Four evaluation factor values in each of 209 grid cells and 7 pumping test hydrologic boreholes (which constituted 216 assessment samples) were collected using the basic functions of data acquisition in the Golden Software Surfer 13.0 to establish a 216 × 4 decision matrix, $D_{216 \times 4}$. Thus, a weighted

normalized decision matrix was established through normalizing and weighting of the decision matrix V as follows:

$$V = (v_{pi})_{216 \times 4} = (W_i \times c_{pi})_{216 \times 4}, \tag{9}$$

$$c_{pi} = d_{pi} / \sqrt{\sum_{p=1}^{216} d_{pi}^2}, \tag{10}$$

where W_i is the total weight of the i th evaluation factor as shown in the third column in Table 4; d_{pi} , indicating the collection value of the p th assessment sample's i th evaluation factor, is the element of the decision matrix $D_{216 \times 4}$; and c_{pi} indicates the normalized value of the p th assessment sample's i th evaluation factor. $i = 1, 2, 3, 4$; $p = 1, 2, \dots, 216$.

Then, based on the weighted normalized decision matrix, NIS and PIS for the water yield property were determined by Hayaty et al. (2014):

$$V^- = \left\{ \left(\max_{1 \leq p \leq l} v_{pi} \mid i \in J_1 \right), \left(\min_{1 \leq p \leq l} v_{pi} \mid i \in J_2 \right) \right\}, \tag{13}$$

$$V^+ = \left\{ \left(\min_{1 \leq p \leq l} v_{pi} \mid i \in J_1 \right), \left(\max_{1 \leq p \leq l} v_{pi} \mid i \in J_2 \right) \right\}, \tag{14}$$

where V^- and V^+ are the negative ideal solution and positive ideal solution, respectively; J_1 indicates the set of negative factors, including BD ; and J_2 is the set of positive factors, including WIB , FIF and DFC .

The distance of each assessment sample to the negative and positive ideal solutions was calculated by the following Eqs. (15)–(16):

$$D_p^+ = \sqrt{\sum_{i=1}^4 (v_{pi} - v_i^+)^2} \tag{15}$$

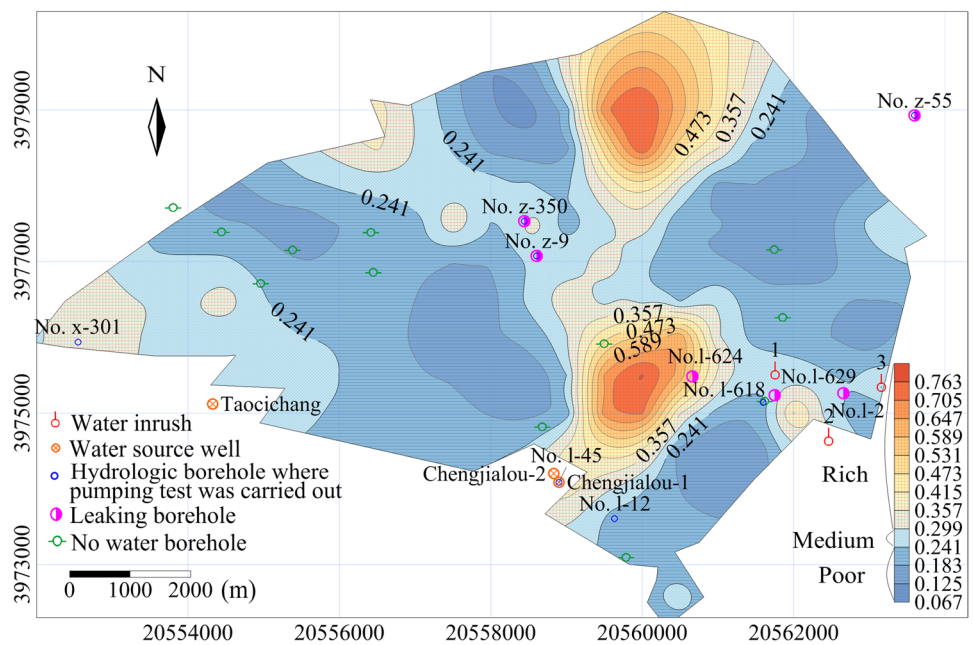
$$D_p^- = \sqrt{\sum_{i=1}^4 (v_{pi} - v_i^-)^2}. \tag{16}$$

Finally, the water yield property index of each assessment sample was calculated as:

$$WYPI_p = \frac{D_p^-}{D_p^+ + D_p^-} \tag{17}$$

where $WYPI_p$ is the water yield property index of the p th assessment sample. The larger the value of $WYPI$ is, the richer the water yield property of the Ordovician top aquifer.

Fig. 4 Water yield property zone map of the Ordovician top aquifer based on the WYPI



Results and discussion

Results

The WYPI was calculated for each grid cell and each pumping test hydrologic borehole. The data were then processed using the Golden Software Surfer 13.0. Based on the coordinates and the WYPI values of the grid cell, the WYPI contour map was established using the kriging function interpolation technique, as shown in Fig. 4. The water yield property of the Ordovician top aquifer as expressed by the WYPI value ranged in the study area from 0.014 to 0.766. Based on the geometric mean method of the seven pumping tests’ WYPI values, the area was divided into three water yield property zones (Fig. 4):

- (a) Poor water yield property zone: $WYPI < 0.232$.
- (b) Medium water yield property zone: $0.232 \leq WYPI < 0.332$.
- (c) Rich water yield property zone: $WYPI \geq 0.332$.

As shown in Fig. 4, in the Ordovician top aquifer, poor water yield property areas are mainly distributed in the southwestern and northeastern areas of the study area; the medium water yield property areas are mainly distributed in the central and southwestern areas of the study area; and the rich water yield property areas are mainly distributed in the north-central, south-central and southwestern parts of the study area.

Validating the prediction of the WYPI model

After obtaining the prediction result, the next step was validation, which was key to verifying the results. Therefore, validation tests were carried out to verify the accuracy of the water yield property zone prediction based on WYPI for the study area by processing practical engineering data, including pumping tests, water inrushes, water source wells, and leakage characteristics of the Ordovician top aquifer.

Analysis of the pumping tests

There were seven pumping tests for the Ordovician top aquifer, listed in Fig. 4. Based on the value of q , the water yield properties of no. l-12 and no. l-618 hydrologic boreholes were classified as poor; nos. z-9, z-350, and z-55 hydrologic boreholes were classified as medium; and nos. x-301 and l-45 were classified as rich (Table 1). As shown in Fig. 4, the

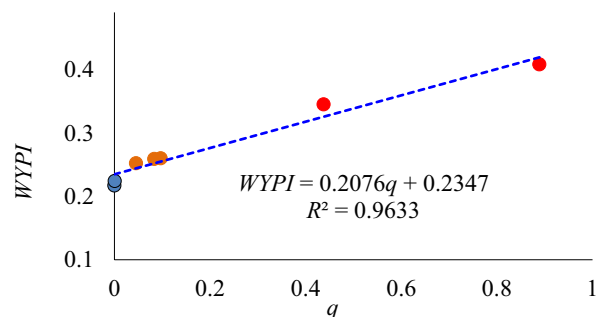


Fig. 5 Scatterplot of q versus WYPI

prediction results based on WYPI are consistent with the data for these seven pumping tests.

Figure 5 involves the scatter plot of WYPI and q . This figure shows that the R^2 was 0.9633, indicating a high degree of fitting between WYPI and q .

Distribution of water intrushes and water source wells

As shown in Fig. 4, no. 2 water intrush, whose water inflow was as high as 1920 m³/h, lies in the rich water yield property zone based on the WYPI. The nos. 1 and 3 water intrushes, whose water inflows were as high as 772.2 m³/h and 78 m³/h, respectively, lie in the medium water yield property zone based on the WYPI.

Located in the southwestern part of the Liangzhuang coalmine, two water source wells (Chengjialou-1 and Chengjialou-2), whose supply is from the Ordovician top aquifer, are the main source of this coalmine. These two water source wells with a 2400 m³/day water supply are located in the rich water yield property zone based on the WYPI (Fig. 4). The Taocichang water source well is also the Ordovician top aquifer water source well, located south of the Xiezhuang coalmine. This water source well with a 1250 m³/day water supply is located in the medium water yield property zone based on the WYPI (Fig. 4).

Therefore, the distributions of the three water intrushes and three water source wells are in agreement with the WYPI prediction.

Leakage characteristic of the Ordovician top aquifer

There were 67 surface boreholes that revealed the Ordovician limestone aquifer, of which 49 boreholes were not taken into consideration because their thicknesses were small. Six of the remaining 18 boreholes, located in the medium or rich water yield property zone based on the WYPI, had leakage issues (Fig. 4). The remaining 12 boreholes had no leakage,

and 11 of these were located in the poor water yield property zone based on the WYPI. However, one borehole with no leakage was located in the rich water yield property zone based on the WYPI. Data from 17 boreholes were consistent with the WYPI prediction, and data from one borehole was not consistent with the WYPI prediction (Table 5). Therefore, the accuracy of the WYPI model was 94.4% based on these 18 boreholes.

Based on the analysis of the distribution of three water intrushes and three water source wells and the leakage characteristics of the 18 surface boreholes, only one prediction result from the WYPI was not consistent with practical engineering data, so the prediction accuracy based on the WYPI was 95.8%. A WYPI prediction is considered to be accurate and reliable and can be used to guide the process of dewatering or other water control measures.

Comparison of the predictions by the WYPI model, q , and the linear regression model

Comparison of the predictions by the WYPI and q

The specific field q , obtained by a pumping test, is traditionally and widely used to evaluate the water yield property of an aquifer in China based on regulations for mine water prevention and control (State Administration of Work Safety and State Administration of Coal Mine Safety 2009). Figure 2 shows the water yield property zone of the Ordovician top aquifer based on q . As shown in Fig. 2, nos. 1, 2, and 3 water intrushes are located in the poor water yield property zone, which is not consistent with practical engineering; three water source wells are located in the rich water yield property zone, which is consistent with practical engineering; nine surface boreholes without leakage occur in the rich or medium water yield property zones; and three surface boreholes with leakage are located in the poor water yield property zone, which is not consistent with practical

Table 5 Water leakage of Ordovician top aquifer in different boreholes

Boreholes	Degree of leakage	WYPI prediction results	WYPI and field results comparison	Boreholes	Degree of leakage	WYPI prediction results	WYPI and field results comparison
No. z-350	Severely	Medium	Agree	No. x-17-1	No	Poor	Agree
No. z-9	Severely	Medium	Agree	No. x-17-2	No	Poor	Agree
No. z-55	Severely	Medium	Agree	No. x-15-3	No	Poor	Agree
No. l-624	Severely	Rich	Agree	No. x-234	No	Rich	Disagree
No. l-629	Slightly	Medium	Agree	No. x-9	No	Poor	Agree
No. l-2	Severely	Medium	Agree	No. l-s12	No	Poor	Agree
No. x-13-2	No	Poor	Agree	No. l-93-3	No	Poor	Agree
No. x-238	No	Poor	Agree	No. l-703	No	Poor	Agree
No. x-12-1	No	Poor	Agree	No. l-713	No	Poor	Agree

Table 6 Normalized data of q and the evaluation factors in seven hydrologic boreholes and the prediction results by least squares

No.	Hydrologic boreholes	Evaluation factors				q	LR
		WIB	FIF	DFC	BD		
1	No. l-12	0.022	0.016	0.041	0.031	0.000226	0.0059352
2	No. l-618	0.036	0.053	0.051	0.07	0.000716	-0.0294181
3	No. l-45	0.079	0.052	0.113	0.03	0.888862	0.8668037
4	No. x-301	0.072	0.046	0.092	0.054	0.437651	0.474619
5	No. z-9	0.024	0.087	0.051	0.071	0.045196	0.0723492
6	No. z-350	0.036	0.081	0.051	0.069	0.083362	0.0700198
7	No. z-55	0.031	0.076	0.072	0.094	0.096921	0.0924612

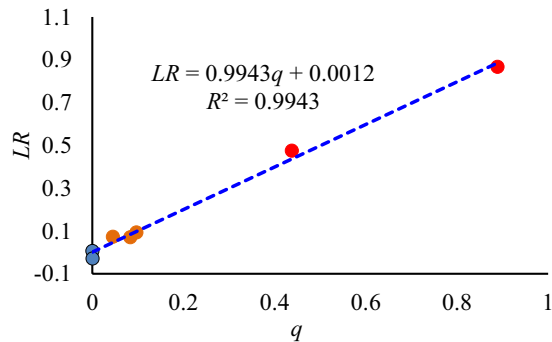


Fig. 6 Scatterplot of q versus LR

engineering. Based on these data, the prediction accuracy based on q is only 37.5%. The prediction accuracy based on the WYPI is 95.8%, indicating that the WYPI performed better than q .

Comparison of the predictions by the WYPI and the linear regression model

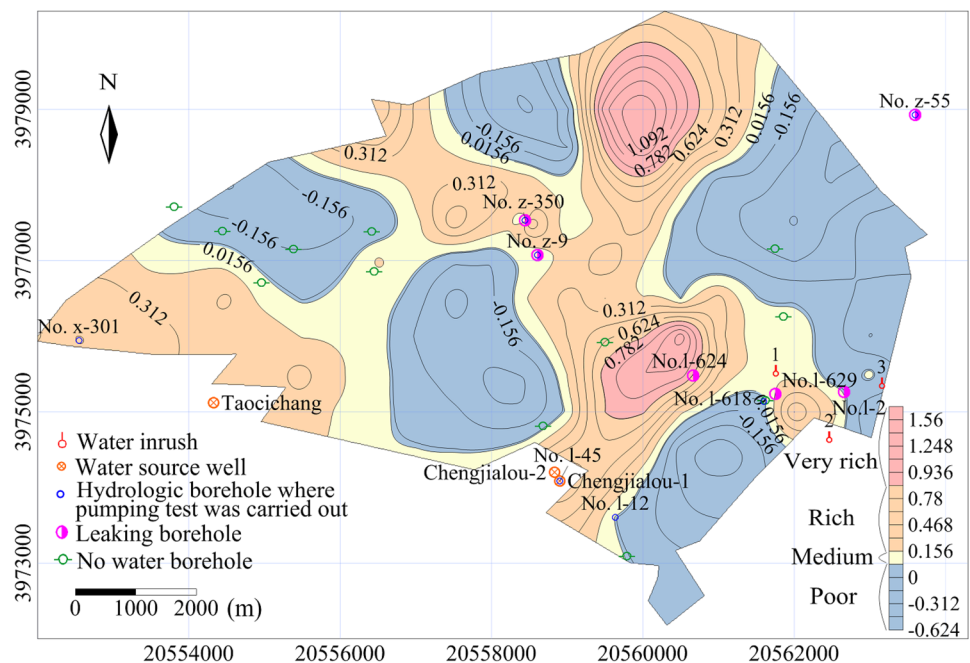
Another simple method is a linear regression model of the water yield property, which was solved by the least square method based on the normalized data in Table 6, as shown in the following:

$$LR = a_1 \times WIB + a_2 \times FIF + a_3 \times DFC + a_4 \times BD + e = 0.3418 \times WIB + 3.3114 \times FIF + 9.9369 \times DFC - 6.7187 \times BD - 0.2537, \tag{18}$$

where LR is the water yield property calculated by the linear regression model; $a_1, a_2, a_3,$ and a_4 are the weights of WIB, FIF, DFC, and BD, respectively; and e is the error.

Table 6 shows the prediction results of LR. Figure 6 is the scatter plot of LR and q . Figure 7 is the water yield property zone map of the Ordovician top aquifer based on LR.

Fig. 7 Water yield property zone map of the Ordovician top aquifer based on LR



From the prediction results (Table 6, Figs. 5, 6), the following can be concluded:

a. The correlation coefficient R^2 is 0.9943 (Fig. 6), indicating that the linear fit of the model is good. However, we can see that the prediction value of the no. 2 sample in Table 6 is negative, and this situation is widespread in the prediction results (Fig. 7). A total of 89 of 216 samples were predicted to be negative, ranging from -0.571 to -0.005 . The predictions do not match actual values.

b. Apart from the above-noted problem, validation tests were carried out to verify the accuracy of the linear regression model by three water inrushes, three water source wells, and the leakage characteristics of 18 surface boreholes.

As shown in Fig. 7, there are three water inrushes and three water source wells, of which the no. 3 water inrush lies in the poor water yield property zone. The prediction accuracy of the linear regression model is 83.3% based on the distributions of the water inrushes and water source wells. Four surface boreholes without leakage are in the rich or medium water yield property zones, and two surface boreholes with leakage are located in the poor water yield property zone. The prediction accuracy of the linear regression model is 66.7% based on these 18 surface boreholes. Therefore, the prediction accuracy based on LR is 70.8% given all the test data. The prediction accuracy based on the WYPI is 95.8%, indicating that the WYPI is more accurate and realistic than LR.

Discussion

Predicting the water yield property of the Ordovician top aquifer is a challenging and difficult task because of deep burial depths and complex geo-circumstances. The water yield property of the Ordovician top aquifer mainly depends on three aspects: the storage space of water, the quantity of water in the storage space, and the water supply. Four factors, WIB, FIF, DFC, and BD, were identified, spatially interpolated, plotted with Golden Software Surfer 13.0, and analyzed. The weights of the four factors were 0.262, 0.227, 0.257, and 0.254, respectively.

WIB intuitively reflects the quantity of water in a storage space. Its weight was 0.262, indicating that WIB has a significant influence on the water yield property. In the south-central and north-central regions, the water inflow of the borehole is larger than that in other regions, and the WYPI is also larger in these regions.

The storage spaces of the Ordovician karst water are mainly cracks and dissolved fissures. FIF indicates the development degree of the cracks and fissures partly, but some of the fissures are filled at a late stage. DFC was adopted to reflect the connectivity of the fissures. Therefore, these two factors comprehensively reflect the development and connectivity of the fissure. Although the weight of the FIF

or DFC is not large, the sum of the two factors' weights is 0.484, which indicates that the development and connectivity of the storage space of water have the greatest influence on the water yield property. The WYPI map shows that faults have a great influence on the water yield property of the Ordovician top aquifer. In the southern part of the study, faults mainly strike to the NE, extending to the south mountain, where the Ordovician limestone strata are exposed to the surface. The distribution direction of the rich water yield property zones based on the WYPI is also the NE direction. The strike of the faults in the deep areas is mainly in the NW direction, which is similar to the distribution direction of the water yield property zone of the Ordovician top aquifer as well. As shown in Fig. 4, the distribution of the Ordovician top aquifer water yield property is very inhomogeneous. Rich water yield property zones are mainly located in the northern and central-eastern part of the study area where faults are developed or intersected densely. Poor water yield property zones are mainly located in regions where faults are not developed.

The weight of BD is 0.254 indicating that water supply has relatively little effect on the water yield property of the Ordovician top aquifer. Storage space has the greatest influence on the water yield property. Controlled by faults, the underground water flows from south of the mountain to the deep part of the study area along the faults.

Based on the WYPI method, a water yield property evaluation of the Ordovician top aquifer was achieved. Practical engineering data, including from seven pumping tests, three water inrushes, three water source wells, and leakage characteristics of 18 surface boreholes, successfully validated the WYPI model. The proposed model was established based on multi-influencing factors of the water yield property that performed better in predicting the water yield property zone of the Ordovician top aquifer than the q and LR methods. The prediction results of the WYPI depend on the abundance of geological and hydrogeological exploration data and will change with the quantity and distribution of all the influential factors. With additional data, the quality of the WYPI prediction will be further improved.

Conclusions

It is essential to assess the water yield property of the Ordovician top aquifer to manage and ensure safe mining in deep coal seams. Due to a minimal number of pumping tests for the Ordovician top aquifer, accurately predicting the water yield property zone was a challenging task. A WYPI model was applied to predict the water yield property zone of the Ordovician top aquifer in the Xinwen coalfield, in which four factors, including water inflow of borehole, fault impact factor, drilling fluid consumption and burial depth of the

Ordovician top aquifer, were used. The GRA and FAHP methods were combined to determine the weights of each factor. The weights of the four factors, WIB, FIF, DFC, and BD, were 0.262, 0.227, 0.257, and 0.254, respectively. The development and connectivity of the storage space of water (FIF and DFC) had the greatest influence on the water yield property. WIB also had a significant influence on the water yield property, followed by BD.

A water yield property zone map was built based on the WYPI using the kriging function interpolation technique. The water yield property zones were divided into three zones: poor ($WYPI < 0.232$), medium ($0.232 \leq WYPI < 0.332$), and rich ($WYPI \geq 0.332$). Practical engineering data, including the water inrushes, water source wells, and leakage characteristics of the Ordovician top aquifer, were used to verify the accuracy of the water yield property zone prediction of the WYPI. The prediction accuracy of the WYPI was 95.8%, while the prediction accuracy of the q and LR methods were 37.5% and 70.8%, respectively. Compared to the prediction results of the q and LR methods, the prediction result of the WYPI model is more consistent with the practical engineering data, which provided guidance on dewatering or other water control measures.

The case study of the Xinwen coalfield shows that the water yield property of the Ordovician top aquifer was predicted with good precision based on the new comprehensive method. The new method can be applied to predict the water yield property of the Ordovician top aquifer for other underground mines in North China where pumping tests are lacking. Notably, the specific relevant factors should be derived from datasets collected in a particular coal mine, because the geological and hydrological conditions are very different in different regions, and then, the method used in this study can be used to establish a similar model for that specific coal mine.

Acknowledgements The authors thank the editors and three anonymous reviewers for their careful work and thoughtful suggestions. We also gratefully acknowledge the financial support of the National Natural Science Foundation of China (51804184, 41572244, 41807283), the Open Fund Research Project of State Key Laboratory of Mining Disaster Prevention and Control Co-founded by Shandong Province and the Ministry of Science and Technology (MDPC2017ZR05), the Scientific Research Foundation of Shandong University of Science and Technology for Recruited Talents (2017RCJ033).

References

- Ataei M, Mikaeil R, Hoseinie SH, Hosseini SM (2012) Fuzzy analytical hierarchy process approach for ranking the sawability of carbonate rock. *Int J Rock Mech Min Sci* 50:83–93. <https://doi.org/10.1016/j.ijrmms.2011.12.002>
- Bu L, Li S, Shi S, Li L, Zhao Y, Zhou Z, Nie L, Sun H (2019) Application of the comprehensive forecast system for water-bearing structures in a karst tunnel: a case study. *Bull Eng Geol Environ* 78(1):357–373. <https://doi.org/10.1007/s10064-017-1114-4>
- Dar IA, Sankar K, Dar MA (2010) Remote sensing technology and geographic information system modeling: an integrated approach towards the mapping of groundwater potential zones in Hardrock terrain, Mamundiyar basin. *J Hydrol* 394:285–295. <https://doi.org/10.1016/j.jhydrol.2010.08.022>
- Deng J (1982) Control problems of grey systems. *Syst Control Lett* 1(5):288–294. [https://doi.org/10.1016/S0167-6911\(82\)80025-X](https://doi.org/10.1016/S0167-6911(82)80025-X)
- Deng J (1989) Introduction to grey system theory. *J Grey Syst* 1(1):1–24
- Gao W, Shi L, Zhai P (2019) Water detection within the working face of an underground coal mine using 3D electric resistivity tomography (ERT). *J Environ Eng Geophys* 24(3):497–505. <https://doi.org/10.2113/JEEG24.3.497>
- Han C, Pan XH, Li GL, Tu JN (2012) The fuzzy analytic hierarchy process of water abundance of an aquifer based on GIS and multi-source information fusion techniques. *Hydrogeol Eng Geol* 39(4):19–25 (in Chinese)
- Hayaty M, Tavakoli Mohammadi MR, Rezaei A, Shayestehfar MR (2014) Risk assessment and the ranking of metals using FDAHP and TOPSIS. *Mine Water Environ* 33(2):157–164. <https://doi.org/10.1007/s10230-014-0263-y>
- Hwang CL, Yoon K (1981) Multiple attributes decision making methods and applications. Springer, Berlin
- Li LP, Zhou ZQ, Li SC, Xue YG, Xu ZH, Shi SS (2015) An attribute synthetic evaluation system for risk assessment of floor water inrush in coal mines. *Mine Water Environ* 34:288–294. <https://doi.org/10.1007/s10230-014-0318-0>
- Li ZX, Wang DD, Lv DW, Li Y, Liu H, Wang P, Liu Y, Liu J, Li D (2018) The geologic settings of Chinese coal deposits. *Int Geol Rev* 60:548–578. <https://doi.org/10.1080/00206814.2017.1324327>
- Mourzenko VV, Thovert JF (2011) Permeability of isotropic and anisotropic fracture networks, from the percolation threshold to very large densities. *Phys Rev E* 84:036307. <https://doi.org/10.1103/PhysRevE.84.036307>
- Qiu M, Shi LQ, Teng C, Zhou Y (2017) Assessment of water inrush risk using the fuzzy delphi analytic hierarchy process and grey relational analysis in the Liangzhuang coal mine, China. *Mine Water Environ* 36(1):39–50. <https://doi.org/10.1007/s10230-016-0391-7>
- Shi L, Qiu M, Wang Y, Qu X, Liu T (2019a) Evaluation of water inrush from underlying aquifers using a modified water-inrush coefficient model and water-inrush index model: a case study in Feicheng coalfield, China. *Hydrogeol J* 27:2105–2119. <https://doi.org/10.1007/s10040-019-01985-2>
- Shi L, Wang Y, Qiu M, Gao W, Zhai P (2019b) Application of three-dimensional high-density resistivity method in roof water advanced detection during working stope mining. *Arab J Geosci* 12(15):464. <https://doi.org/10.1007/s12517-019-4586-7>
- Shi S, Wei J, Xie D, Yin H, Li L (2019c) Prediction analysis model for groundwater potential based on set pair analysis of a confined aquifer overlying a mining area. *Arab J Geosci* 12(4):115. <https://doi.org/10.1007/s12517-019-4267-6>
- State Administration of Work Safety, State Administration of Coal Mine Safety (2009) Regulations for mine water prevention and control. China Coal Industry Publishing House, Beijing, Beijing (in Chinese)
- Sun W, Wu Q, Liu H, Jiao J (2015) Prediction and assessment of the disturbances of the coal mining in Kailuan to karst groundwater system. *Phys Chem Earth* 89–90:136–144. <https://doi.org/10.1016/j.pce.2015.10.008>
- Wang D, Shi L (2019) Source identification of mine water inrush: a discussion on the application of hydrochemical method. *Arab J Geosci* 12(2):58. <https://doi.org/10.1007/s12517-018-4076-3>

- Wang X, Meng FB (2018) Statistical analysis of large accidents in China's coal mines in 2016. *Nat Hazards* 92:311–325. <https://doi.org/10.1007/s11069-018-3211-5>
- Wu Q (2014) Progress, problems and prospects of prevention and control technology of mine water and reutilization in China. *J China Coal Soc* 39(5):795–805 (in Chinese)
- Wu Q, Fan ZL, Liu SQ, Zhang YW, Sun WJ (2011a) Water-richness evaluation method of water-filled aquifer based on the principle of information fusion with GIS: water-richness index method. *J China Coal Soc* 36(7):1124–1128 (in Chinese)
- Wu Q, Xing LT, Ye CH, Liu YZ (2011b) The influences of coal mining on the large karst springs in North China. *Environ Earth Sci* 64:1513–1523. <https://doi.org/10.1007/s12665-009-0376-y>
- Wu Q, Xu H, Pang W (2008) GIS and ANN coupling model: an innovative approach to evaluate vulnerability of karst water inrush in coalmines of north China. *Environ Geol* 54:937–943. <https://doi.org/10.1007/s00254-007-0887-3>
- Wu GJ, Chen WZ, Yuan JQ, Yang DS, Bian HB (2017a) Formation mechanisms of water inrush and mud burst in a migmatite tunnel: a case study in China. *J Mt Sci* 14(1):188–195. <https://doi.org/10.1007/s11629-016-4070-8>
- Wu Q, Jiang L, Wu Q (2017b) Study on the law of mining stress evolution and fault activation under the influence of normal fault. *Acta Geodyn Geomater* 14(3):357–369. <https://doi.org/10.1016/j.ijrmm.2014.05.021>
- Wu Q, Xu K, Zhang W, Wei Z (2017c) Roof aquifer water abundance evaluation: a case study in Taigemiao, China. *Arab J Geosci* 10:254. <https://doi.org/10.1007/s12517-017-3048-3>
- Xu D, Shi L, Qu X, Tian J, Wang K, Liu J (2019) Leaching behavior of heavy metals from the coal gangue under the impact of site ordovician limestone karst water from closed shandong coal mines, North China. *Energy Fuels* 33(10):10016–10028. <https://doi.org/10.1021/acs.energyfuels.9b01928>
- Xue Y, Gao F, Liu XG (2015) Effect of damage evolution of coal on permeability variation and analysis of gas outburst hazard with coal mining. *Nat Hazards* 79:999–1013. <https://doi.org/10.1007/s11069-015-1888-2>
- Xu K, Zhang W, Shen JJ, Dk Z, Li B (2016) Fissured aquifer water yield capacity evaluation based on fractal dimension and weighted grey relational degree theory. *J Liaoning Tech Univ (Nat Sci)* 35(8):816–820 (in Chinese)
- Yan J (2015) Water yield property assessment for zhiluo formation lower member aquifer in Hongliu coalmine, Ningxia. *Coal Geol China* 28(30):45–49 (in Chinese)
- Yang C, Liu SD, Wu RX (2017) Quantitative prediction of water volumes within a coal mine underlying limestone strata using geophysical methods. *Mine Water Environ* 36:51–58. <https://doi.org/10.1007/s10230-016-0394-4>
- Yin H, Shi Y, Niu H, Xie D, Wei J, Lefticariu L, Xu X (2018) A GIS-based model of potential groundwater yield zonation for a sandstone aquifer in the Juye Coalfield, Shangdong, China. *J Hydrol* 557:434–447. <https://doi.org/10.1016/j.jhydrol.2017.12.043>
- Yin H, Zhao H, Xie D, Sang S, Shi Y, Tian M (2019) Mechanism of mine water inrush from overlying porous aquifer in Quaternary: a case study in Xinhe Coal Mine of Shandong Province, China. *Arab J Geosci* 12(5):163. <https://doi.org/10.1007/s12517-019-4325-0>
- Zhang S, Guo W, Li Y (2017) Experimental simulation of water-inrush disaster from the floor of mine and its mechanism investigation. *Arab J Geosci* 10(22):503. <https://doi.org/10.1007/s12517-017-3287-3>
- Zhao TB, Zhang ZY, Tan YL, Shi C, Wei P, Li Q (2014) An innovative approach to thin coal seam mining of complex geological conditions by pressure regulation. *Int J Rock Mech Min Sci* 71:249–257. <https://doi.org/10.1016/j.ijrmm.2014.05.021>
- Zhao TB, Guo WY, Tan YL, Yin YC, Cai LS, Pan JF (2018) Case studies of rock bursts under complicated geological conditions during multi-seam mining at a depth of 800 m. *Rock Mech Rock Eng* 51:1539–1564. <https://doi.org/10.1007/s00603-018-1411-7>

Publisher's Note Springer Nature remains neutral with regard to jurisdictional claims in published maps and institutional affiliations.